

# An S-FSCW Based Multi-Channel Reader System for Beamforming Applications using Surface Acoustic Wave Sensors

Clemens PFEFFER<sup>1</sup>, Stefan SCHEIBLHOFFER<sup>(1)2</sup>, Reinhard FEGER<sup>1</sup>, Andreas STELZER<sup>1,3</sup>

<sup>1</sup> Christian Doppler Laboratory for Integrated Radar Sensors, Altenbergerstr. 69, 4040 Linz, Austria

<sup>2</sup> Hainzl Industriesysteme, Industriezeile 56, 4021 Linz, Austria

<sup>3</sup> Inst. for Communications Engineering and RF-Systems, Johannes Kepler Univ., Altenbergerstr. 69, 4040 Linz, Austria

c.pfeffer@nthfs.jku.at, s.scheiblhofer@hainzl.at, r.feger@nthfs.jku.at, a.stelzer@nthfs.jku.at

**Abstract.** *Interrogating multiple surface acoustic wave (SAW) sensors located within the same radar beam require techniques to separate the multiple superposing SAW sensor responses. The presented multi-channel reader features four parallel transceiver channels, which are based on the switched frequency-stepped continuous-wave principle and high-speed parallelized baseband electronics. Thus classical beamforming applications including angle of arrival measurement of single SAW tags and the angular separation of multiple SAW sensors are presented and compared to a multiple-input multiple-output (MIMO) approach. Due to the larger virtual array in the MIMO approach a larger aperture can be synthesized, which leads to significantly better angular separation results. The level analysis for the given system is verified by baseband-power measurements at different readout distances, considering the hardware parameters as well as the free-space propagation aspects. Finally measurements assess the maximum interrogation distance for the system.*

## Keywords

S-FSCW, SAW-tag, multi-channel reader system, beamforming, MIMO, AOA.

## 1. Introduction

Surface acoustic wave (SAW) based delay lines are suitable in many industrial applications to measure physical quantities, such as temperature, pressure, and strain, or for identification issues [1], [2], [3]. These sensors are commonly interrogated in the frequency domain, using radar principles, such as the frequency-modulated continuous-wave or frequency-stepped continuous-wave (FSCW) concept. In [4] we recently introduced the application of digital beamforming (DBF) methods using a single-channel reader hardware in combination with multiplexed antennas to calculate the angle-of-arrival (AOA), from the measured tag responses. With the DBF approach it is possible to

separate multiple sensors, even if they are located within the interrogation beam simultaneously (Fig. 1). Not only that DBF minimizes the collision effects of superposing responses of multiple sensors, but also the tag's position can be evaluated.

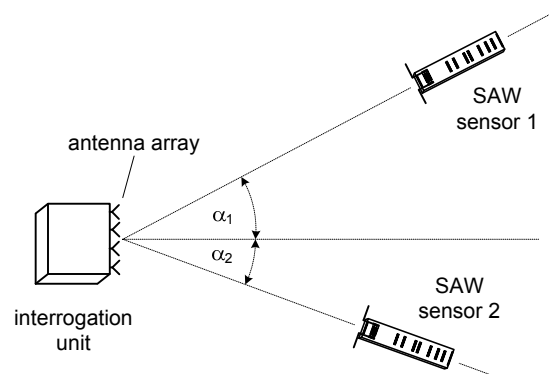


Fig. 1. Tag separation using beamforming methods.

In [5] a 4-channel reader unit with distinct RF and baseband channels has been developed and introduced to shorten measurement times compared to sequential single-channel measurement method described in [4]. This leads to improved accuracy for the AOA measurements, especially in dynamic scenarios, where the sensor is moving during the readout. Extending the results of [5], in this work a more detailed explanation of the used signal model and the necessary simplifications will be presented. Additional measurement results demonstrate the maximum readout distance and standard deviation for the measured angle and a level analysis for the interrogation system verify the reader unit performance.

## 2. A Multi-Channel SAW Reader

Fig. 2 illustrates a block diagram of the 4-channel reader unit, which operates in the 2.45 GHz industrial-scientific-medical (ISM) band. To achieve a simultaneous sensor readout on all receive channels, the RF-frontend is parallelized and drives a quad-channel baseband unit,

which is controlled by a field-programmable gate array (FPGA). All RF-channels are driven coherently from a PLL-based signal source via a classical power splitter. The design is divided into an analog (light gray) and a digital (dark gray) section. Digital isolators are used for all control signals connecting the baseband and RF-board. For further reuse of the baseband board the IF-interconnection is done by SMA-cables (blue, dashed dotted).

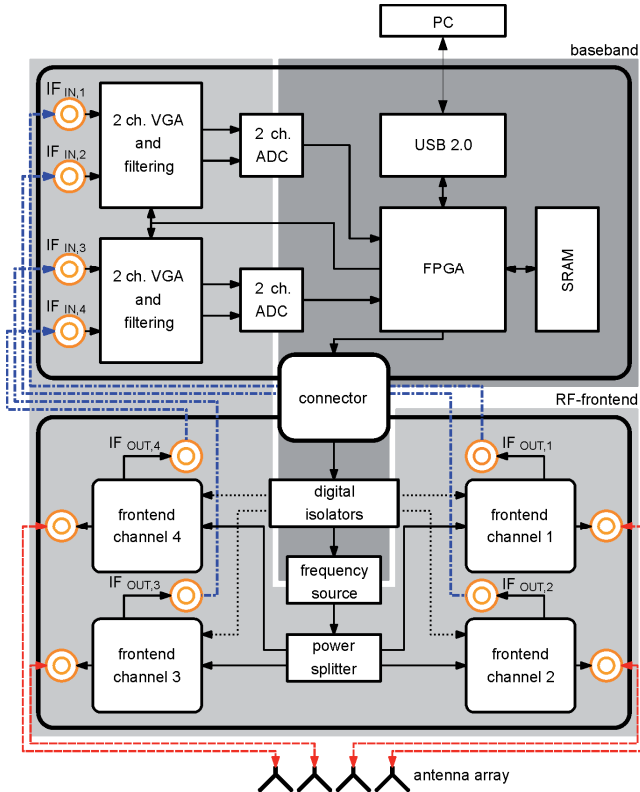


Fig. 2. Block diagram of the 4-channel reader unit.

2.1 RF-Frontend

A schematic of a single frontend channel can be seen in Fig. 3. The frontend concept is based on the switched-FSCW (S-FSCW) principle [6, 7], which implements a temporal gating scheme for both, transmit and receive signals using two RF switches. Due to this technique, excellent suppression of leakage signals, especially from the antenna’s mismatch as well as environmental interference at low round-trip delay-times (RTDTs) can be achieved by temporal masking.

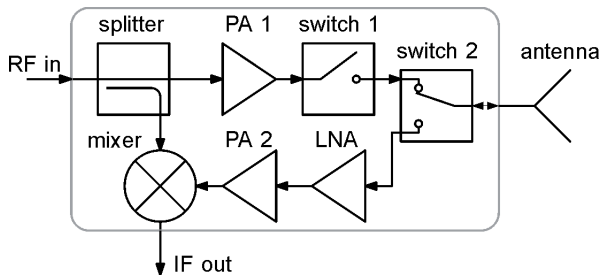


Fig. 3. Detail of a frontend channel.

Depending on the switch configuration, each channel can operate in transmitter, receiver, or transceiver mode. The output power at the antenna interface can be controlled via the variable power amplifier (PA1) and achieves a maximum of +20 dBm. A programmable low-noise amplifier (LNA) with a followed power amplifier (PA2) in the receiving path deliver a gain of up to 40 dB. Setting the LNA gain to nearly the maximum value the overall RF-frontend gain in the receiving path was +28 dB, considering the mixer’s conversion loss of 6 dB and an insertion loss of 1.6 dB for the switch (switch 2).



Fig. 4. Photograph of the quad-channel SAW reader.

2.2 Baseband Hardware

In the quad-channel baseband stage the IF-signals from the receive mixers are amplified, filtered, and fed to 14-bit differential 25 MSps analog to digital converters (ADCs). The amplification and single-ended to differential conversion is realized by two programmable dual channel gain amplifiers. The timing critically sampling and switching process as well as the system control is realized in an Altera Cyclone III FPGA. All timing related processes are implemented in VHDL-programmed hardware blocks. A softcore processor controls and configures the system and starts the interrogation process. During the measurement process the sampled data is stored in a SRAM and transferred afterwards to the PC via a high-speed USB2.0 interface. A photograph of the interrogation printed circuit board with a total board size of

200x160 mm<sup>2</sup> is shown in Fig. 4. The board shape is defined by the intended enclosure.

### 2.3 Level Analysis RF-/IF-Stage

At room temperature the insertion loss of the used SAW-tags is about -40 dB to -45 dB depending on the construction of the sensor. In combination with the path loss the interrogation unit has to detect very low power levels at the receivers mixer output. Tab. 1 lists the level plan for a typical measurement setup used to interrogate SAW-tags in a distance of 2.5 m.

TX power (EIRP)	+10 dBm
Single path loss	-48 dB
Tag antenna gain	+8 dBi
SAW sensor loss	-45 dB
Tag antenna gain	+8 dBi
Single path loss	-48 dB
RX antenna gain	+8.5 dBi
RF-frontend gain	+28 dB
Total power and amplitude level from SAW-tag response at the input of the IF-path	-78.5 dBm -88.5 dBV
IF-frontend gain	+16 dB
IF-amplitude of SAW-tag response at the input of the ADC	-72.5 dBV

Tab. 1. Level analysis for the given system.

## 3. MIMO Beamforming Principle

### 3.1 Signal Model

Each of the frontend channels is connected to an antenna, which are arranged as an antenna array. In the classical beamforming approach, the antennas are spaced equidistantly, which results in a four-element uniform linear array (ULA) configuration, as shown in Fig. 5. The phase information in each received signal is different due to the different propagation delays, if the reflected wave coming from the SAW sensor impinges onto the array from an angle other than  $\alpha = 0^\circ$ .

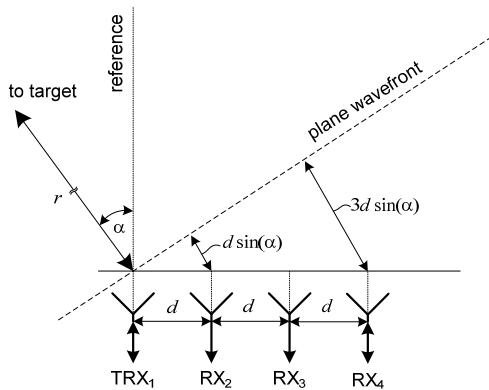


Fig. 5. Beamforming principle, using a four-element physical ULA, with channel 1 as transceiver (TRX) and channels 2 to 4 as receivers (RX).

Assuming a single SAW sensor with  $p$  reflectors located in the array's farfield which, according to [8] begins at

$$r_{ff} = \frac{2D^2}{\lambda}, \quad (1)$$

the resulting digitized IF signal  $s_{IF}[n, m]$  can be stated as:

$$s_{IF}[n, m] = \sum_{i=1}^p A_i \cos \left( 2\pi \left( f_0 \frac{2r_i + dm \sin(\alpha)}{c_0} + \frac{B}{N} \frac{2r_i + dm \sin(\alpha)}{c_0} n \right) + \phi_{0_i} \right) \quad (2)$$

Here,  $A_i$  denotes the signal amplitude,  $f_0$  the sweep start frequency,  $d$  the antenna separation,  $r_i$  the range with respect to the reference point,  $c_0$  the speed of light, and  $\phi_{0_i}$  the reflection phase. The index  $n = 0$  to  $N-1$  is the temporal sampling index, with  $N$  the total number of samples per IF channel,  $m = 0$  to  $M-1$  is the spatial sampling index, with  $M$  the total number of receive channels. In (1)  $\lambda = c_0/f_0$  denotes the wavelength and  $D$  the maximum size of the antenna array. To separate the temporal and spatial indices in (2) which simplifies the signal model, the bandwidth  $B$  has to satisfy the narrowband assumption (see [9]), therefore it is necessary that:

$$\frac{4DB}{c_0} \leq 1. \quad (3)$$

Assuming a single SAW sensor to be located in the array's far field, which results in plane wave fronts and the limitation (3) on the used interrogation bandwidth  $B$  to hold, the resulting digitized IF signal (2) can be approximated as

$$s_{IF}[n, m] \approx \sum_{i=1}^p A_i \cos \left( 2\pi \left( \frac{f_0}{c_0} dm \sin(\alpha) + \frac{B}{N} \frac{2r_i}{c_0} n \right) + \phi_{0_i} \right) \quad (4)$$

Since the dependencies on the temporal and spatial indices  $n$  and  $m$  are separated in (4), the range and angular information can now be extracted from the measurement data separately using a two-dimensional fast Fourier transform (FFT).

### 3.2 MIMO Approach

Since in the reader system all frontend channels are capable of being used as a transmitter, it is possible to synthesize a larger virtual array via a multiple-input multiple-output (MIMO) approach, as introduced in [10]. This is achieved by performing two consecutive measurements using transmitter 1 for the first and transmitter 4 for the second readout. Due to the spatial offset of antenna 4 with respect to the array reference and the resulting phase offset regarding the transmitted signal, three additional virtual receiver position are generated, as it is indicated in Fig. 6. The resulting seven-element virtual array yields a larger aperture and consequently a smaller beam width thus

leading to a better angular separation capability. The theoretical zero-to-zero beam width  $\theta_0$  can be calculated by [11]

$$\theta_0 = \frac{2\lambda}{dM \cos(\alpha)}, \quad (5)$$

thus, the application of the MIMO principle improves the angular separability of two sensors by a factor of 1.75.

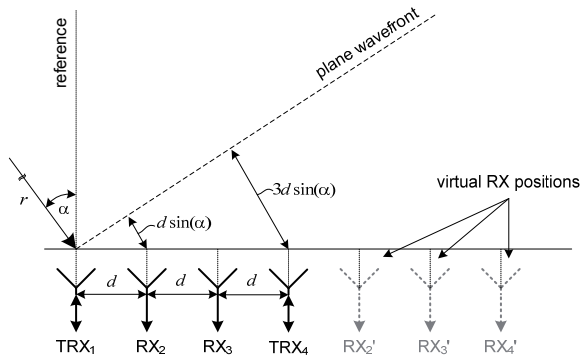


**Fig. 6.** MIMO principle, generating a seven-element virtual ULA from a four-element physical ULA by consecutively using channel 1 and channel 4 in transmit mode.

If additionally the inner channels 2 and 3 are used as transmitters in the ULA configuration, redundant virtual channels are generated, which can be used for averaging purposes or – in non-static scenarios – for target velocity estimation.

## 4. Measurements

The reader operates in the 2.45 GHz ISM band and uses a bandwidth of  $B = 83.5$  MHz, with a starting frequency of  $f_0 = 2.40$  GHz. Per channel  $N = 801$  data points are sampled. The effective isotropically radiated output power is configured to +10 dBm, to comply with federal regulations. The reader system is equipped with commercially available planar antennas, providing a gain of 8.5 dBi. The antennas are placed in an ULA configuration, with a minimum possible separation of  $d = 85$  mm, which is defined by the antenna's housing. According to (2) the virtual seven antenna array's size  $D = 6 \cdot 85$  mm = 510 mm together with  $\lambda = 0.12$  m leads to  $r_{ff} \approx 4.25$  m. Note that at lower distances the propagating wave front is spherical rather than plane, which causes a distortion of the otherwise linearly increasing phase along the array. In the targeted application the readout range starts at 2.5 m. This results in a maximum angle deviation of less than  $1^\circ$  (at  $\alpha_{max} = 40^\circ$ ), compared to the plane wave assumption, thus causing only minor angular offsets, which are neglected as second order imperfection in the following. As another effect, the larger aperture leads to a smaller beamwidth and so to better angular separation results. Due to the antenna spacing of larger than  $\lambda/2$  the unambiguous angular region is decreased and therefore the AOA measurements are limited to  $\pm 40^\circ$ , which comply with the targeted applica-

tion. Considering the required usage of the given antennas the measurement results show that this setup fulfills the desired performance.

### 4.1 SAW-Tag Separation

In the first measurement scenario, two SAW identification (ID) tags with eight reflectors each, located at the same range of 2.5 m but at an angular separation of  $22^\circ$  are interrogated. Fig. 7 shows an overlay of the resulting superposed tag responses at all seven virtual array channels, which are calculated via an FFT (zeropadding factor:  $2^{17}$ , window function: Hanning). Since some reflectors, e.g. the framing reflectors, on both tags are located at nearly the same position, effects of constructive and destructive interference can be observed.

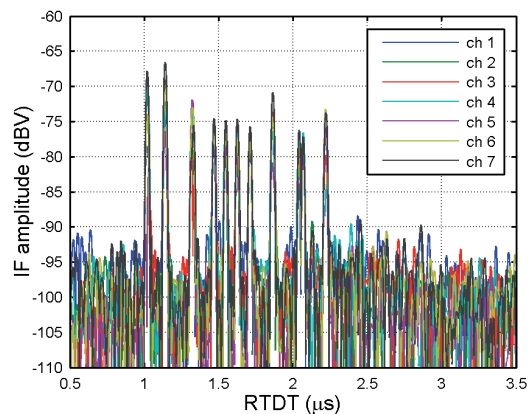


**Fig. 7.** IF spectra of two superposing SAW sensors, with 8 reflectors each, at a distance of 2.5 m and an angular separation of  $22^\circ$ .

In Fig. 8 the beamforming result for the data from Fig. 7 is calculated, using the four physical array channels only. As can be seen at the well separated reflectors, it is obvious that there are two responses coming from different AOAs, but due to the relatively broad beam width of  $\theta_0 = 41.2^\circ$  the tags cannot be separated clearly. However, if the MIMO principle is applied, the beam width reduces to  $\theta_0 = 23.5^\circ$  for  $M = 7$ . Consequently, the tags' responses separate, which is illustrated in Fig. 9.

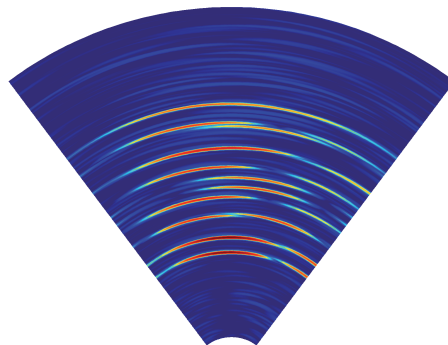


**Fig. 8.** DBF result of interrogating two SAW sensors at a range of 2.5 m, separated by  $22^\circ$ , using the standard 4-channel ULA configuration.

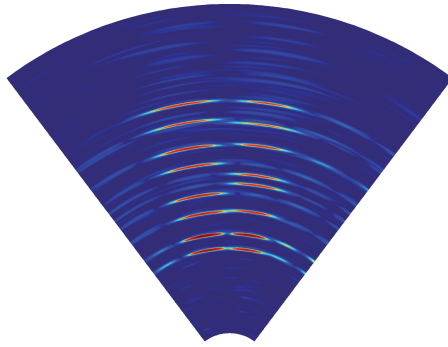


Fig. 9. Improved DBF result using the 4-channel ULA to synthesize a 7-channel virtual array, using the MIMO approach.

### 4.2 Angle-of-Arrival Measurement

In the second measurement setup, the interrogation unit is mounted on a computer controlled turn table. In this configuration, a single SAW tag at a distance of 2.5 m is interrogated, while rotating the antenna array in steps of 5° around the arrays reference point. The measured tag angles in Fig. 10 as well as the deviation in Fig. 11 show a measurement error of less than 1°.

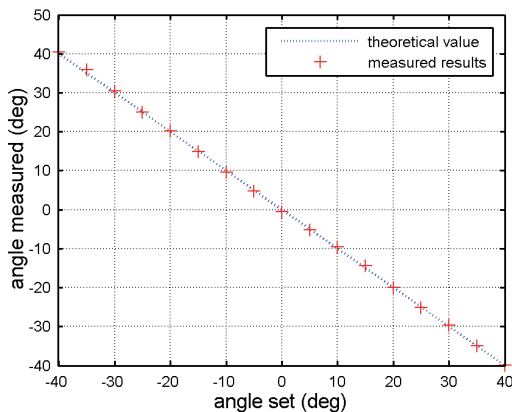


Fig. 10. Measured versus set angle, interrogating a SAW sensor at a distance of 2.5 m with the reader mounted on a turn table.

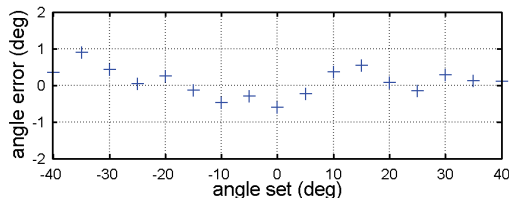


Fig. 11. Deviation of set and measured rotation angle.

### 4.3 Measurement of Angular Standard Deviation

In the third measurement setup, a single SAW tag is placed 2 m in front of the interrogation unit at an angle of 0°. The angle histograms of 100 interrogations of the

SAW-tag’s second (Fig. 12) and seventh reflector (Fig. 13) are evaluated and show a Gaussian distribution. Due to the lower Signal to Noise Ratio (SNR) of reflector 7, the distribution is widened, indicating the increased variance.

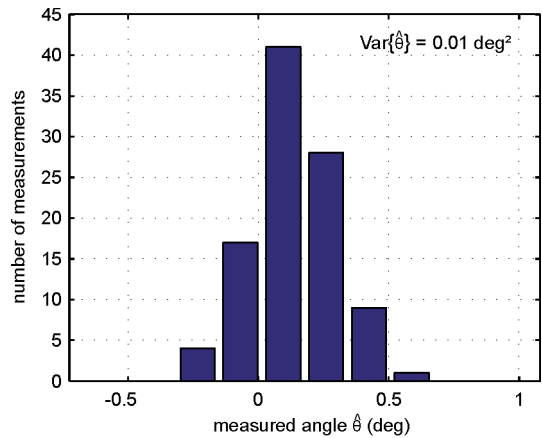


Fig. 12. Angle histogram of the second reflector for 100 interrogations.

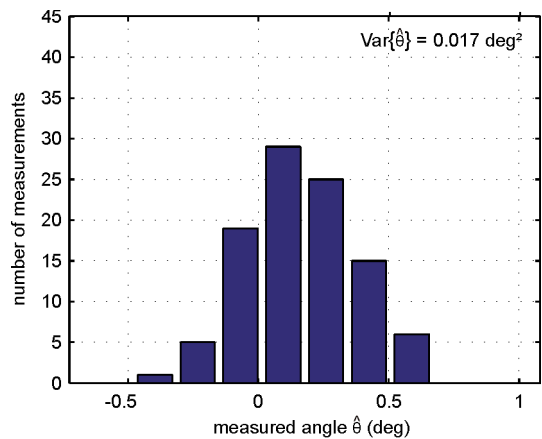


Fig. 13. Angle histogram of the seventh reflector for 100 interrogations.

In the next measurement setup, a single SAW tag is placed on 3 different positions with different distances and angles. For 100 measurements of the second reflector the standard deviations  $\sigma$  of the angle are listed in Tab. 2.

Position	Range (m)	Amplitude (dBV)	Angle (deg)	$\sigma$ (deg)
1	3.5	-78.5	0.2	0.16
2	4	-80.5	14.8	0.17
3	4.5	-83.0	-19.3	0.18

Tab. 2. Angle standard deviation  $\sigma$  at three different measurement positions.

As expected the measurement results show that the angle deviation increases with lower SNR.

### 4.4 Power Levels at Different Distances

To determine the maximum interrogation distance, measurements of the reflector with the highest IF-power levels were taken at distances from 1 m to 8 m in steps of

1 m at  $0^\circ$ . The results of the measured IF-power levels are shown in Fig. 14. The levels match the solid line which is derived from the radar-equation taking into account the IF-power at 2.5 m of  $-72.5$  dBV as calculated in Tab.1. The dashed line denotes the bound where the spectral signal peak level to noise level is 15 dB. Thus the useful maximum readout distance should be limited to 5 m. Exemplary two SAW sensor responses at readout distances of 1 m and 3 m are shown in Fig. 15 and Fig. 16. Additional disturbances caused by multi-reflections [7] of the SAW-tag can be observed in Fig.15 compared to Fig. 16. They lead to increased level of disturbances as can be observed in Fig. 15.

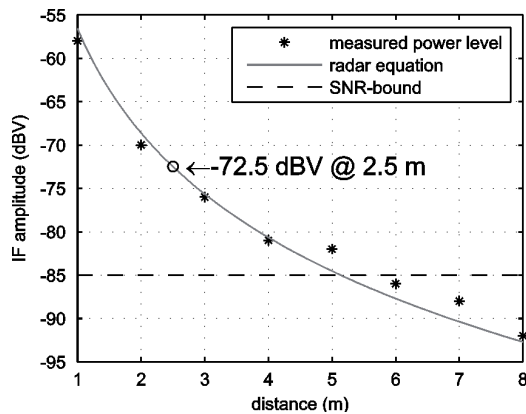


Fig. 14. Measured IF-power versus radar-equation.

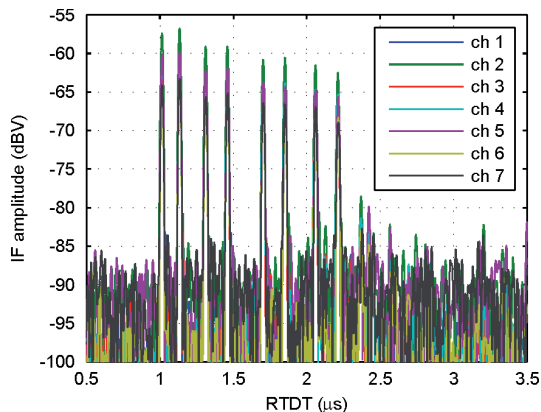


Fig. 15. IF spectra of SAW sensor response at a distance of 1 m.

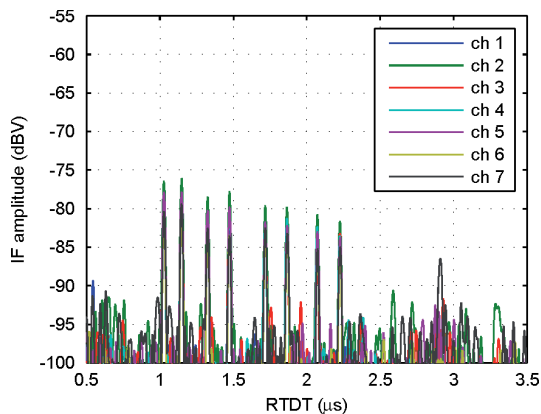


Fig. 16. IF spectra of SAW sensor response at a distance of 3 m.

## 5. Conclusion

In this paper we presented a multi-channel SAW reader system on applications of SAW tag separation and angle measurement. The parallelized frontend structure achieves a four times faster readout, compared to the sequential single-channel measurement method. Due to the flexible transceiver architecture used for the RF-channels, a larger virtual array can be realized by transmitter switching using the MIMO principle. This approach significantly improves the angular separation performance. Further the measurement results show that it is possible to achieve sub-degree angle accuracy. A detailed level analysis verified by range measurements determines a reasonable maximum readout distance of 5 m.

## Acknowledgements

The authors wish to acknowledge the Austrian Center of Competence in Mechatronics for partly sponsoring this work.

## References

- [1] KALININ, V. Passive wireless strain and temperature sensors based on SAW devices. In *Proceedings of the IEEE Radio and Wireless Conference*. Atlanta (USA), September 2004, p. 187 - 190.
- [2] HARTMAN, C. A global SAW ID tag with large data capacity. In *Proceedings of the IEEE Ultrason. Symp.* Munich (Germany), October 2002, p. 65 - 69.
- [3] POHL, A. A review of wireless SAW sensors. *IEEE Transactions on Ultrasonics, Ferroelectrics and Frequency Control*, March 2000, vol. 47, no. 2, p. 317 - 332.
- [4] STELZER, A., SCHEIBLHOFER, S., SCHUSTER, S., BRANDL, M. Multi reader/multi tag SAW RFID systems combining tagging, sensing and ranging for industrial applications. In *Proceedings of the International Frequency Control Symposium*. Honolulu (USA), May 2008, p. 263 - 272.
- [5] SCHEIBLHOFER, S., PFEFFER, C., FEGER, R., STELZER, A. An S-FSCW based multi-channel reader system for beamforming applications using surface acoustic wave sensors. In *Proceedings of the Conference ICECom 2010*. Dubrovnik (Croatia), September 20-23, 2010, p. 1 - 4.
- [6] SCHEIBLHOFER, S., SCHUSTER, S., STELZER, A. Modelling and performance analysis of SAW reader systems for delay-line sensors. *IEEE Transactions on Ultrasonics, Ferroelectrics and Frequency Control*, October 2009, vol. 56, no. 10, p. 2293 - 2303.
- [7] SCHEIBLHOFER, S., SCHUSTER, S., STELZER, A., HAUSER, R. S-FSCW-radar based high resolution temperature measurement with SAW sensors. In *Proceedings of the 6<sup>th</sup> International Symposium on Signals, Systems, and Electronics (ISSSE'04)*. Linz (Austria), August 10-13, 2004, p. 128 - 131.
- [8] BALANIS, C. A., *Antenna Theory: Analysis and Design*. 3<sup>rd</sup> ed. Hoboken, NJ: Wiley, 2005.
- [9] FEGER, R., WAGNER, C., SCHUSTER, S., SCHEIBLHOFER, S., STELZER, A. Accuracy improvement for direction of arrival

estimation by use of a mirror element. *IEEE Transactions on Microwave Theory and Techniques*, April 2011, vol. 59, no. 4, p. 1016 - 1024.

- [10] FEGER, R., WAGNER, C., SCHUSTER, S., SCHEIBLHOFER, S., JÄGER, H., STELZER, A. A 77-GHz FMCW MIMO radar based on a SiGe single-chip transceiver. *IEEE Transactions on Microwave Theory and Techniques*, May 2009, vol. 57, no. 5, p. 1020 - 1035.
- [11] TREES, H. L. *Detection, Estimation, and Modulation Theory, Part IV, Optimum Array Processing*. New York, NY: Wiley Interscience, 2002.

## About Authors ...

**Clemens PFEFFER** was born in St. Pölten, Austria, in 1975. He received the Dipl.-Ing. (M.Sc.) degree in Mechatronics from Johannes Kepler University, Linz, Austria, in 2009. In 2009, he joined the Institute for Communications and Information Engineering, Johannes Kepler University, as a Research Assistant and became a member of the Christian Doppler Laboratory for Integrated Radar Sensors, Johannes Kepler University.

**Stefan SCHEIBLHOFER** was born in Linz, Austria, in 1979. He received the Dipl.-Ing. (M.Sc.) degree in Mechatronics in 2003 and the Dr. techn. (Ph.D.) degree in Mechatronics in 2007, all from the Johannes Kepler University, Linz, Austria. Since 2007 he was working at the Christian Doppler Laboratory for Integrated Radar Sensors within the Institute for Communications and Information Engineering, Johannes Kepler University, Linz, Austria. 2010 he moved to Hainzl Industriesysteme as a key researcher.

His primary research interests concern advanced radar system concepts, development of radar signal processing algorithms, statistical signal processing, RF design, and its application to automotive radar and surface acoustic wave sensor applications.

**Reinhard FEGER** was born in Kufstein, Austria, in 1980. He received the Dipl.-Ing. (M.Sc.) degree in Mechatronics and Dr. techn. (Ph.D.) degree in Mechatronics from Johannes Kepler University, Linz, Austria, in 2005 and 2010, respectively. In 2005, he joined the Institute for Communications and Information Engineering, Johannes Kepler University, as a Research Assistant. In 2007, he became a member of the Christian Doppler Laboratory for Integrated Radar Sensors, Johannes Kepler University.

He is a reviewer for international journals and conferences. His research topics are radar signal processing, as well as radar system design for industrial and automotive radar sensors. Dr. Feger was recipient of the 2011 Microwave Prize and the 2011 German Microwave Conference (GeMiC) Best Paper Award.

**Andreas STELZER** received the Diploma Engineer degree from the Technical University of Vienna, Vienna, Austria, in 1994, and the Dr. techn. degree (Ph.D.) from the Johannes Kepler University, Linz, Austria, in 2000.

In 2003 he became Associate Professor at Johannes Kepler University. Since 2007, he has been Head of the Christian Doppler Laboratory for Integrated Radar Sensors, and since 2011 he is full Professor at Johannes Kepler University, heading the department for RF-Systems. He has authored or coauthored over 245 journal and conference papers. His research is focused on microwave sensor systems for industrial and automotive applications, RF and microwave subsystems, surface acoustic wave sensor systems, as well as digital signal processing for sensor signal evaluation.

Dr. Stelzer received several awards including the IEEE COM Innovation Award and the European Microwave Association (EuMA) Radar Prize in 2003. He was also the recipient of the 2011 German Microwave Conference (GeMiC) Best Paper Award as well as of the 2008 IEEE Microwave Theory and Techniques Society (IEEE MTT-S) Outstanding Young Engineer Award and the 2011 IEEE Microwave Prize.